Deformation characteristics of rubber sphere aggregates and sand-tire chips mixtures in triaxial compression condition

Kikuchi, Y.
Port & Airport Research Institute, Yokosuka, Japan

Sato, T.
Kumamoto University, Kumamoto, Japan

Hazarika, H.
Akita Prefectural University, Ugohonjo, Japan

Hidaka, T.
Toa Corporation, Yokohama, Japan

Keywords: drained triaxial compression test, rubber sphere, tire chip-sand mixture, X-ray CT scanner

ABSTRACT: In this paper, we discuss the deformation characteristics of sand-tire chips mixtures. Deformation characteristics of tire chips or rubber sphere aggregates were observed. And we found that the tire chip specimen or the rubber sphere aggregate was only compressed and was less sheared during triaxial compression. The deformation characteristics of a mixture of sand and tire chips were greatly affected by the deformation characteristics of tire chips.

1 INTRODUCTION

Earth pressure acting on quay wall structures can be reduced if tire chips are used for the backfill (Kaneda et al. 2007). But, it is a problem that tire chips have high compressibility and deform easily. To prevent this problem, consideration is being given to using tire chips mixed with sand. In this paper, a series of drained triaxial compression tests of rubber sphere specimen was conducted to find a basic deformation and shear strength feature of a mixture of sand and tire chips,. Investigations into the compressibility of the rubber sphere specimen and deformation of rubber sphere particles were conducted via X ray CT scanning. Then a series of triaxial tests on the specimen mixture of sand and tire chips was conducted and the characteristics of shear strength and compressibility of the mixture were discussed.

2 DEFORMATION CHARACTERISTICS OF RUBBER SPHERE AGGREGATE AND TIRE CHIP AGGREGATE

A series of drained triaxial compression tests were conducted to investigate the deformation characteristics of tire chips during compressive shearing.

2.1 *Experimental methods*

The particle density of rubber spheres was 1.270 g/cm^3, with a diameter of 8.0 mm. The tire chips used were derived from used tires, with metal and fibers removed beforehand, by crushing them with a machine into smaller pieces measuring a maximum of 2 mm in diameter. The particle density thereof was 1.150 g/cm^3, with maximum and minimum void ratios of 1.632 and 1.091, respectively. Rubber spheres and tire chips were washed with a detergent to remove impurities adhered to their surfaces and then dried.

The diameter and the height of the specimen were 5 cm and 10 cm respectively. The target relative density of the tire chip specimen (TC) was 100%. The number of the rubber sphere particles was controlled to 405 to prepare the rubber sphere aggregate (RS). The consolidation pressures used were 30 and 100 kN/m^2. The void ratios of the specimen after consolidation were 0.4 - 0.5 and 0.2 - 0.3 in consolidation pressures of 30 and 100 kN/m^2 respectively in both TC and RS, although the accuracy of the measured void ratios was low because of membrane penetration. Drained triaxial compression (CD) tests with 1.0% compression strain velocity were conducted.

2.2 *Experimental results*

Figure 1 shows the stress strain relationship of TC and RS. The deviator stress of RS was slightly higher than that of TC at the same axial strain in each consolidation pressure. Except in the case of RS consolidated in 30 kN/m^2, there were no maximum deviator stresses observed until 23% of the axial strain.

These test results show that the deformation characteristics of TC and RS were found to be originally similar. The reason for this similarity is the similarity of the particle deformability of tire chips and rubber spheres.

X-ray CT scanner was used during triaxial tests to observe the particle deformation and the deformation of rubber sphere aggregates. In this case, RS was used instead of TC, because the deformation and relative movement of the particles were more easily observed in RS than in TC.

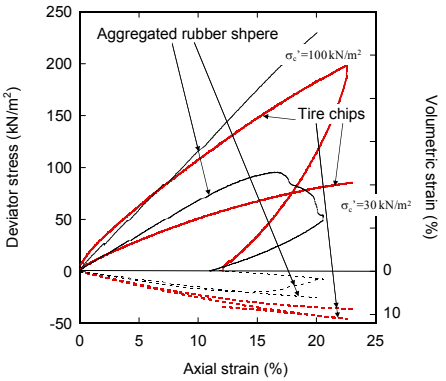

Figure 1. Triaxial test results of TC and RS

Figure 2 shows (a) the X-ray CT image of the deformation of RS during the CD test, with the vertical cross section on the central axis and (b) the stress - strain relationship of the test. In this test, a consolidation pressure of 30 kN/m^2 was used. In both figures, the numbers presented were corresponding. As shown in Fig. 2, monotonic loading was conducted up to an axial strain of 15% which is numbered (4). Up to this step, only a very small lateral deformation of the specimen was observed. Then specimen was unloaded to (5), where the axial strain was about 7%. Up to this state, there were no observations regarding the relative sliding of each particle. But at stage (6), however, the specimen deformed into a barrel shape and shearing-type relative movement of the particles was observed.

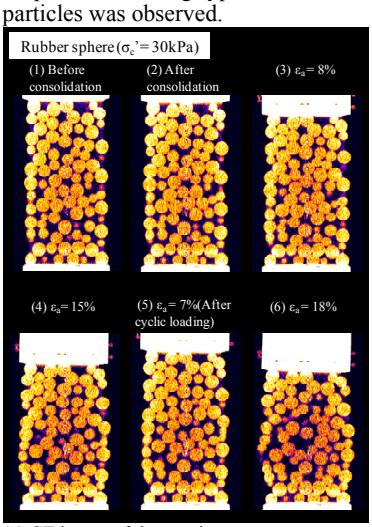

(a) CT image of the specimen.

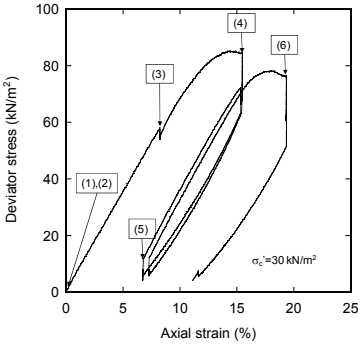

(b) Relation between step number and stress strain condition.

Figure 2. X-ray CT image of the vertical cross section of the specimen during CD compression.

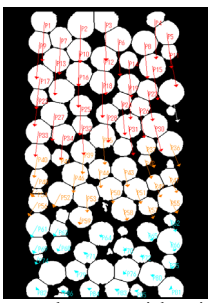

(a) Displacement vectors between axial strains of 0 to 15%.

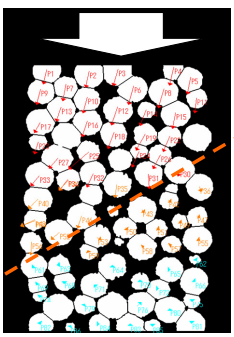

(b) Displacement vectors between axial strains of 15 to 18%.

Figure 3. Particle displacement vectors during each axial strain.

The movement of each particle was traced to observe changes in this deformation mode change. Figure 3 shows the movement of each particle. Particle displacement vectors during axial strain from 0% to 15% are shown in (a), and those during 15% to 18% are shown in (b). As shown in (a), most particles moved nearly vertically up to 15% of axial strain, and particle displacement was large in upper particles and small in lower particles. As shown in (b), the particles in the upper portion moved not only

vertically but also horizontally, even though particles in the lower part seldom moved during axial strain of 15% to 18%. Based on this observation, the surface slid as shown in (b). This shear deformation produced deviator stress reduction and dilative volume strain as shown in Fig. 1.

This kind of dilative deformation was observed only in RS consolidated in 30 kN/m^2 as shown in Fig. 1; this means that compression is the main deformation mode of tire chips in triaxial compression, and shear deformation is seldom observed.

Particle deformation was also observed in RS during the CD test. When the axial load was applied, the RS particles were compressed vertically and expanded horizontally; when the axial load was removed, the RS particles returned to their original shape. This kind of particle deformation affects the compressive deformation of the aggregates.

3 DEFORMATION CHARACTERISITCS OF A MIXTURE OF TIRE CHIPS AND SAND

3.1 *Experimental methods*

Tire chips derived from used tires (ρ_s=1.15 g/cm^3, e_{max}=1.556, e_{min}=1.126, D_{max}=2.0 mm), Sohma sand #4 (ρ_s=2.644 g/cm^3, e_{max}=0.970, e_{min}=0.634, D_{50}=0.77 mm, D_{max}=2.0 mm), and a mixture of these two materials were used in this series of experiments. The tire chips and Sohma sand were mixed in various proportions, with the volume ratios of sand to tire chips set at 10:0, 7:3, 5:5, 3:7, and 0:10. Here, s_f (sand fraction) indicates the proportion by volume occupied by Sohma sand in the tire chip-sand mixture. Thus, s_f =1 indicates samples consisting of sand only.

The specimens used for CD tests were prepared by moist tamping. The tire chips and Sohma sand were mixed at the prescribed ratio, with water added to the mixture to obtain an initial water content of w= 10%. The diameter and height of the specimen were 5 cm and 10 cm, respectively. The specimen was prepared by placing the mixture in five layers, with each layer compacted a prescribed number of times by dropping a rammer from a prescribed height to control the compaction energy to perform the 50% of relative density in the specimen of s_f =1.0. The same amount of compaction energy was applied to each specimen with different sand fractions.

The specimen was saturated and consolidated at a confining pressure of 50 kN/m^2 with a back pressure of 100 kN/m^2, and a drained compression test was conducted with a strain velocity of 1.0%/min. CT scanning was conducted at 2% axial strain increments for s_f =1.0, 0.7, 0.3, 0.0, and at 4% axial strain increments for s_f =0.5.

3.2 *Experiment results*

Figure 3 shows the relationships between stress - axial strain and volumetric strain - axial strain of the triaxial compression test. The solid lines show the stress - axial strain relationship, while the hashed lines show the volumetric strain - axial strain relationship. For the stress - strain curves, the higher the sand fraction, the larger the stress increment ratio and the smaller the strain at the maximum deviator stress. In particular, there was no maximum deviator stress observed for s_f =0.0 until 20% of axial strain. There were no large differences observed in maximum deviator stress except at s_f =0.0. In terms of compressibility, the larger the sand fraction, the larger the dilative tendency.

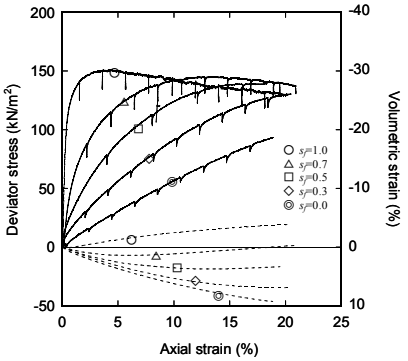

Figure 3. Deviator stress - volumetric strain - axial strain relationship of tire chips - sand mixture.

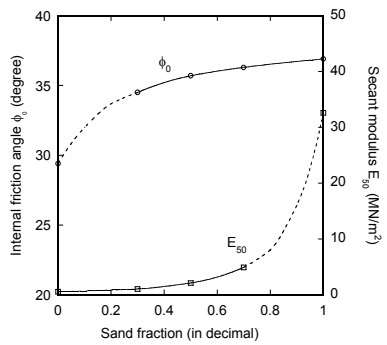

Figure 4. Change of internal friction angle and young modulus by sand fraction.

Figure 4 shows the change of internal friction angle ϕ_0 and young modulus E_{50} by sand fraction. When s_f was larger than 0.3, small differences were observed in ϕ_0, although large reductions of ϕ_0 were observed when s_f =0.0. As for E_{50}, large differences were observed between s_f of 1.0 and 0.7, but differences between s_f of 0.7 and 0.0 were small. This difference of change in ϕ_0 and E_{50} are affected by the deformation characteristics of the mixture. E_{50} is mainly affected by early stages of compression, and

at those stages, deformation characteristics are mainly affected by the compressibility of tire chips. On the other hand, ϕ_0 is affected by the final stage of compression and the final shear strength is mainly affected by the shear resistance of sand.

3.3 *Deformation characteristics of the tire chip-sand mixture observed by X-ray CT scanner*

Figure 5 shows the deformation of the specimens after compression and presents X-ray CT images of the vertical cross section on the specimen's central axis. The images on the upper row show the initial state, and those on the bottom row show the state of at axial strain of 20%. In the images, brightness represents density, with lighter parts having higher density and darker parts having lower density. For s_f =0.7 and 0.3, the images include both darker and lighter parts, with the former being tire chips and the latter being sand particles. When the specimen was compressed to an axial strain of 20%, the specimen with s_f =1.0 was deformed as barrel shape. This kind of horizontal deformation decreased with decrease of sand fraction, and for s_f =0.0, no horizontal deformation was observed.

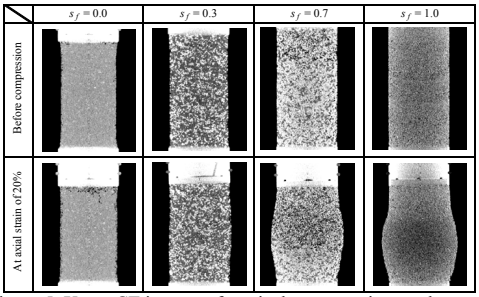

Figure 5. X-ray CT images of vertical cross section on the central axis before and after compression in various sand fractions.

Next, shear strain distribution was observed with the PIV method during compression. Figure 6 shows shear strain distribution calculated from the displacement vector analyzed by the PIV method. In this figure, the darker the section, the higher the shear strain, and there were almost no shear strain observed in white sections.

For the specimen for which s_f =1.0, a clear shear zone was observed at the middle of the specimen at an axial strain of 12%. The shear strain concentrated zone was observed at an axial strain of 20%. This kind of shear strain concentration became indistinctive as sand fraction decreased. And as shown in the case of s_f =0.3, shear strain distribution was almost homogeneous and shear strain level was small.

The deformation characteristics of the specimen changed as a consequence of mixing tire chips with sand. Young's modulus was decreased, shear strain level was decreased, and shear strain concentration was diminished with decreasing sand fraction. However, ultimate shear resistance rarely changed with decreasing sand fraction. These kind of characteristic changes are due to the deformation characteristics of tire chips.

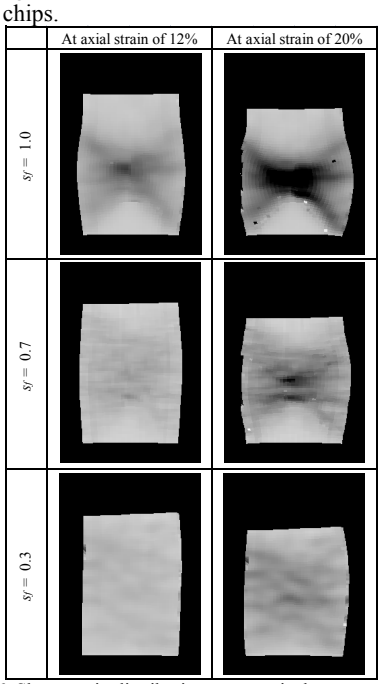

Figure 6. Shear strain distribution on a vertical cross section on the central axis derived from PIV analysis.

4 CONCLUSIONS

In this paper, we discussed the deformation characteristics of a tire chips and sand mixture. We first observed the deformation characteristics of tire chips before discussing the mixture. Based on this observation, the tire chip specimen was only compressed and was less likely to be sheared during triaxial compression.

The deformation characteristics of a mixture of tire chips and sand were different from only sand itself. Young's modulus was decreased, shear strain level was decreased, and shear strain concentration was diminished with decreasing sand fraction. Ultimate shear resistance, however, rarely changed with decreasing sand fraction. These kinds of changes are due to the deformation characteristics of tire chips.

REFERENCE

Kaneda, K., Hazarika, H., & Yamazaki, H. 2007. The numerical simulation of earth pressure reduction using tire chips in backfill, *Scrap Tire Derived Geomaterials*, pp.245-251.